

## THE DUST SURROUNDING W HYDRAE

E. H. WISHNOW<sup>1</sup>, C. H. TOWNES<sup>1</sup>, B. WALP<sup>2</sup>, AND S. LOCKWOOD<sup>1</sup>

<sup>1</sup> Space Sciences Laboratory and Department of Physics, University of California, Berkeley, CA 94720, USA; [wishnow@ssl.berkeley.edu](mailto:wishnow@ssl.berkeley.edu), [cht@ssl.berkeley.edu](mailto:cht@ssl.berkeley.edu)

<sup>2</sup> Gemini Observatory, 670 N. A'ohoku Place, Hilo, HI 96720, USA; [bwalp@gemini.edu](mailto:bwalp@gemini.edu)

Received 2009 September 4; accepted 2010 February 23; published 2010 March 9

### ABSTRACT

Dust shells surrounding the star W Hydrae have been resolved and measured at a wavelength of  $11.15\ \mu\text{m}$ , using the Infrared Spatial Interferometer. Two different models for the star and dust shells are used to fit the data, one for recent data taken over short time spans and another for the combined data of 15 years. Modeling of the data shows the presence of two dust shells with diameters of approximately 100 mas and 250 mas. The inner dust shell is seen to expand over the year 2008. The observations are consistent with a stellar diameter of 50 mas.

*Key words:* stars: general – stars: individual (W Hydrae) – techniques: interferometric

### 1. INTRODUCTION

The asymptotic giant branch (AGB) star W Hydrae, spectral type M7e, has been known for some time to be surrounded by rather dense gas, dust, and active masers. Measurements of the star have been made recently at near infrared wavelengths (Woodruff et al. 2008, 2009) and in the microwave region (Reid & Menten 2007). We report here on detailed measurements at mid-infrared wavelengths, which show a dense and discrete dust distribution. A variety of stellar radii have been previously measured; these vary particularly with wavelength due to effects from the spectra of the surrounding gas. Measurements of dust surrounding the star reported here use a narrow bandwidth which avoids spectral lines.

Measurements of W Hydrae were made with the Infrared Spatial Interferometer (ISI). The interferometer, described by Hale et al. (2000), operates at  $11.15\ \mu\text{m}$  wavelength using  $\text{CO}_2$  lasers as local oscillators, which provide heterodyne detection with a narrow bandwidth ( $0.18\ \text{cm}^{-1}$ ). The lasers are tunable, allowing avoidance of spectral lines and hence direct measurement of the continuum from warm dust and from the star without confusion due to surrounding gas. The ISI consists of three moveable telescopes, arranged for the 2008 and 2009 measurements in an appropriate triangle with baseline separations of about 36 m. This allows measurement from three different directions as well as the closure phase to determine any deviations from a center of symmetry. Measurements made in 1994 and 1999 used a two-telescope system with baselines of 32 m and 4 m, respectively.

### 2. MEASUREMENTS

Measurements of the mid-IR visibility of W Hydrae, obtained during three observation periods, are shown in Figure 1. Data shown in the upper panel were obtained on 2008 February 13 and 27; data shown in the middle panel were obtained on 2008 June 16, 17, and 27; and data shown in the lower panel were obtained on 2009 January 31. In each panel, visibility values for the three differently oriented baselines fit quite well on a smooth curve, indicating little difference in the dust distribution for the three different baseline position angles. In addition, the phase closures measured for the three measurement periods, from top to bottom, are  $0^\circ.5 \pm 7^\circ$ ,  $13^\circ \pm 11^\circ$ , and  $58^\circ \pm 37^\circ$ , indicating that the source is generally centro-symmetric, particularly for the 2008 measurements. The abscissae in Figure 1 give the inter-

ference fringe frequency in spatial frequency units, labeled SFU ( $1\ \text{SFU} = 10^5\ \text{cycles rad}^{-1}$ ). The visibility can be seen to decrease over the SFU range 13 to about 30; a flattening of the visibility curve above 30 SFU is seen in the data of 2008 June and 2009 January. The range of 13–30 SFU corresponds to sinusoidal interferometer response functions with peak separations of approximately  $0''.16$ – $0''.07$ , allowing objects about half this size to be resolved. A dust shell component is therefore resolved and its size is well measured; however, the star, which provides the remaining small visibility above 30 SFU, is not well resolved and hence its size is not well determined by these measurements.

The visibility measurements of Figure 1 are well fitted by a model with two uniform disk (UD) components, one associated with the star and the other with the dust shell. The flattening of the visibility curves for SFUs beyond  $\sim 30$  corresponds to the presence of an object smaller than the dust shell. The stellar diameter at near IR wavelengths was measured as  $42.5 \pm 0.7\ \text{mas}$  (Monnier et al. 2004), but the likelihood of limb darkening was also pointed out. The combined measurements, including two-telescope observations conducted in 1994 June and 1999 June, are shown in Figure 2. These measurements are best fitted with a stellar component UD of 50 mas diameter and this size, though not very accurate, has been used throughout the present work. Although one cannot expect the dust shell to be a discrete disk of completely uniform flux, this model fits the measured visibilities well and must be a reasonably accurate approximation.

The fitting parameters associated with the curves of Figure 1 are given in Table 1. The upper panel of Figure 1 shows that 19% of the total flux comes from a region with an angular extent 50 mas and 39% of the total flux comes from a region with an angular extent of 94 mas. The remaining 42% of the total flux comes from an additional resolved outer dust shell. The presence of this larger shell is demonstrated by earlier visibility measurements (1999 June) at spatial frequencies between 3 and 12 SFU shown in Figure 2. This full data set can be fairly well fitted by a model with three UDs representing the star and two dust shells. The low spatial frequency data points are fitted with a UD curve associated with an angular radius of 189 mas that joins smoothly with the UD curves of the inner shell and the star of Figure 1. These three curves, and their sum, are shown in Figure 2. The fitted curve has a visibility value of 0.96 at zero SFU rather than unity and this indicates that the data are reasonably, but not perfectly, fitted by the model. The

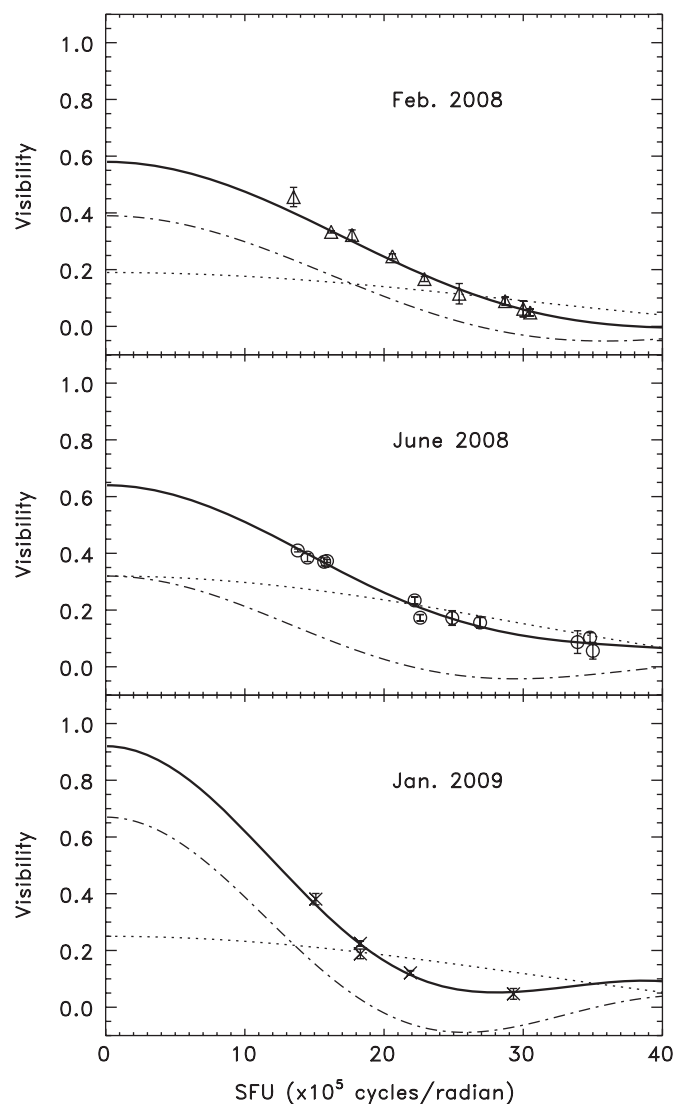


**Figure 1.** ISI visibility measurements of W Hydrae made over three observing epochs. Abscissae are in spatial frequency units (SFU) of  $10^5$  cycles  $\text{rad}^{-1}$ . The visibility is fitted with a model (solid line) consisting of a UD representing the star (dotted line) plus a UD representing the dust shell (dot-dashed line). The fitted parameters are given in Table 1. Visibility of an outer dust shell, more or less completely resolved at  $\text{SFU} > 10$ , represents the remaining intensity.

angular size of the outer dust shell corresponds reasonably well with the  $\sim 150$  mas radius  $\text{H}_2\text{O}$  maser ring observed by Reid & Menten (2007).

A simple model has been used to estimate properties of the star and dust disks from the fitted parameters. The model assumes that the star is a UD which is embedded within inner and outer UDs representing the dust shells. The fractions of the total flux arising from each region are functions of three unknowns:  $T_s$ , the stellar temperature; and  $\tau_1$  and  $\tau_2$ , the optical depths of the inner and outer dust shells. The temperature of a dust shell,  $T_d$ , is estimated from the assumption  $T_d = T_s(R_s/R_d)^{0.5}$ , where  $R_s$  and  $R_d$  are the stellar and dust shell radii, respectively. The total flux of W Hydrae varies within a stellar luminosity cycle and also from cycle to cycle. The total flux at  $11.15 \mu\text{m}$  during each observation period is determined by calibration against flux measurements of Arcturus which is assumed to have an  $11 \mu\text{m}$  flux of 640 Janskys (Monnier et al. 1998).

The results of the model are given in Table 1. The stellar temperature of  $\sim 2100$  K is lower than that expected for a late

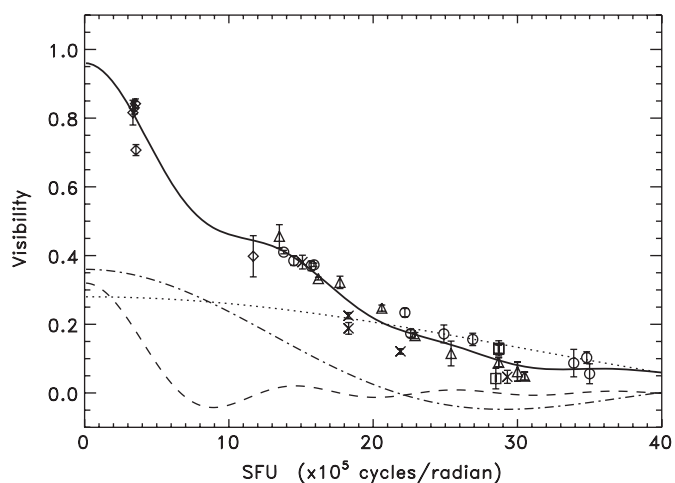


**Figure 2.** Visibility of W Hydrae, combining data over several years and using baselines in different directions. Data from 2008 February are indicated by triangles, 2008 June by circles, 2009 January by crosses, 1999 by diamonds, and 1994 by squares. The data are fitted by a model curve (solid) consisting of three UD curves associated with the star (dotted), an inner (dot-dashed) and an outer dust shell (dashed). The fitted radii (in mas) and fractions of total flux for the three disks are  $25.0$ ,  $0.28 \pm 0.01$ ;  $58.1 \pm 1.7$ ,  $0.36 \pm 0.02$ ;  $189.2 \pm 3.5$ ,  $0.32 \pm 0.05$  (no probable error is given for the stellar radius, since it is not well determined).

stage M star, but the model is simple, and the temperature is consistent with  $2390 \pm 550$  measured at  $7 \text{ mm}$  wavelength (Reid & Menten 2007). Furthermore, since the stellar size is not very accurately determined, it could be 10% smaller which would increase the temperature in this model to  $\sim 2300$  K. Errors in the determinations of the radii and flux fractions (as given in Table 1) result in variations of the model temperatures of  $\sim 10\%$ , optical depths of  $\sim 25\%$ , and transmissivity of the shells of  $\sim 10\%$ .

The stellar luminosity phase is pertinent to the dust visibility curve, since a change in stellar luminosity changes the dust temperature and hence its contributions to visibility. The stellar period during recent years is approximately 387 days (from the All Sky Automated Survey, ASAS), and luminosity phases at the different periods of measurement are noted in Table 1. The visibility values for the different phases differ somewhat, but Figure 1 does not show a strong correlation with luminosity phase. The total flux and temperatures of the star and outer dust shell determined from the model are, however, correlated with luminosity phase. There is a systematic increase in the size of the inner dust shell with time as can be seen by the diminishing of the overall width of the visibility curves in Figure 1 from top to bottom. This is also shown in the fitted values for the inner shell radii in Table 1. The distance to W Hydrae is 104 pc (Whitelock et al. 2008) so the assumed stellar size of  $0''.050$  gives a stellar diameter of 5.2 AU. The variation in the inner dust shell radius of  $0''.047$ – $0''.065$  over the course of about a year gives a radial size variation of 4.9–6.8 AU or a velocity of  $9 \text{ km s}^{-1}$ . Similarly, the fraction of total flux associated with the outer dust shell diminishes with time, indicating that the outer shell is perhaps also expanding and dissipating. There are, however, no measurements at low spatial frequencies during this time period that might show a change in size of the outer dust shell.

Although the visibility measurements at different times and luminosity phases are not expected to agree exactly because of changes in luminosity and dust movement, the data for all observations are fairly consistent. Figure 3 shows all ISI measurements over the time period 1994–2008, where these

**Table 1**  
Parameters Derived From Fits to W Hydrae Data and Model Results<sup>a</sup>

Parameter	Observation Date		
	2008 Feb	2008 Jun	2009 Jan
Stellar luminosity phase	0.1	0.5	0.1
Assumed stellar radius (mas)	25.0	25.0	25.0
Stellar fraction of total flux	$0.19 \pm 0.05$	$0.32 \pm 0.02$	$0.25 \pm 0.02$
Inner dust shell radius (mas)	$47.1 \pm 4.6$	$57.2 \pm 2.7$	$65.4 \pm 2.5$
Inner shell fraction of total flux	$0.39 \pm 0.03$	$0.32 \pm 0.02$	$0.67 \pm 0.08$
Outer dust shell radius (mas)	190.0	190.0	190.0
Outer shell fraction of total flux	0.42	0.36	0.08
Flux ratio compared to Arcturus	$6.68 \pm 0.61$	$5.48 \pm 0.16$	$5.92 \pm 0.48$
Total flux (Jansky)	4275	3507	3789
Results from model			
Optical depth of inner dust shell	0.36	0.16	0.33
Optical depth of outer dust shell	0.055	0.040	0.009
Stellar temperature	2125	2063	2129
Temperature of inner dust shell	1550	1366	1320
Temperature of outer dust shell	771	748	772
Transparency of the inner dust shell	0.70	0.85	0.72
Transparency of the outer dust shell	0.95	0.96	0.99

**Notes.**

<sup>a</sup> Parameters from W Hydrae measurements and model results for the three periods of observation shown in Figure 1. The stellar and inner dust shell radii and fractions of total flux are from the UD curves shown in Figure 1. The outer dust shell radius is obtained from the combined data shown in Figure 2; its fraction of total flux brings to unity the sum of the stellar and disk fractions. The model assumes the star is a UD embedded within inner and outer dust disks with uniform luminosities. Transparency of the inner shell refers to  $11.15 \mu\text{m}$  light from the star; transparency of the outer shell refers to light from the star and inner dust shell. Errors in the temperatures and shell transparencies are  $\sim 10\%$ .

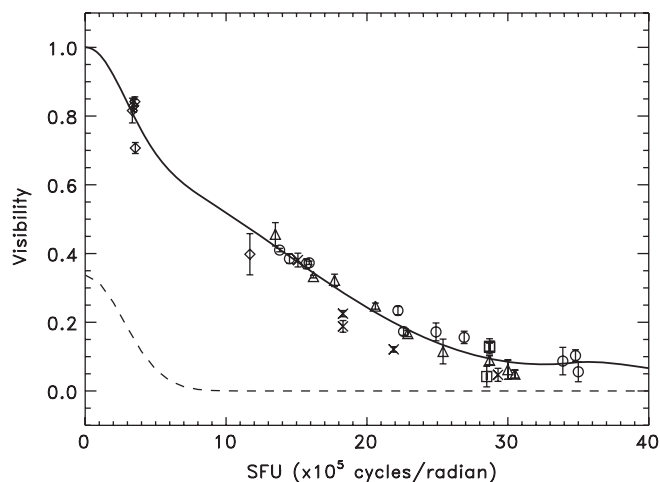


**Figure 3.** Visibility of W Hydrae, combining data over several years and using baselines in different directions. Data from 2008 February are indicated by triangles, 2008 June by circles, 2009 January by crosses, 1999 by diamonds, and 1994 by squares. A smooth curve has been fitted to the data (solid) with a Gaussian component for the outer dust shell (dashed).

are the same data presented in Figure 2. In order to determine the radial distribution of material around the star with minimal reference to a particular time or model, the entire data set has been fitted with a smooth curve shown in Figure 3. A Gaussian component associated with the outer dust shell is shown by the dashed line, indicating that it is well resolved at SFUs  $\geq 10$ . The Fourier transform of this smooth visibility curve, extended to high spatial frequencies using a UD of 50 mas diameter for the star, gives the one-dimensional integrated intensity profile shown in Figure 4. This fitting procedure follows that of Tatebe et al. (2006), with the exception that in the present case the

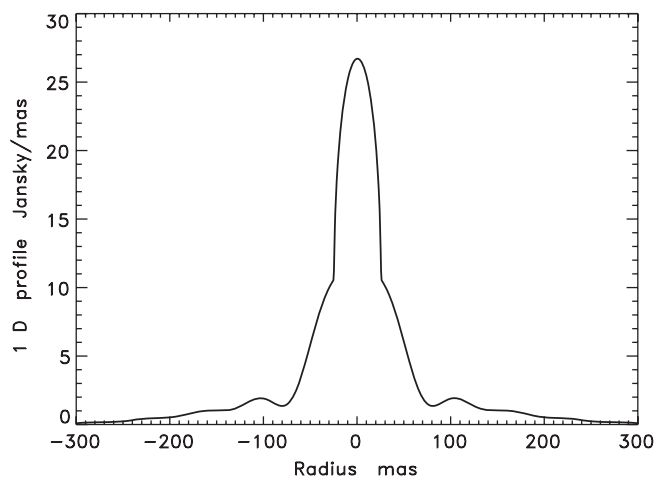


**Figure 4.** Intensity profile of W Hydrae obtained from the full visibility data set shown in Figure 3. The intensity is plotted as a function of distance from the center of the star. Dust shells at average radii of approximately 40 mas and 150 mas can be seen. The larger shell diminishes gradually in intensity with increasing radius.

closure phase is considered to be zero. The one-dimensional profile shows the central star surrounded closely by the inner dust shell and an outer dust shell with a peak at a radius of 110 mas that diminishes gradually with increasing radius. The profile is an approximation to the real situation, but it fits the data rather well and gives an overall picture for the star and surrounding distribution of dust.

As noted earlier, the apparent diameter of W Hydrae has been previously measured at a number of wavelengths where these values vary substantially because of the material surrounding the star. Aperture mask interferometry at the Keck telescope

over a wavelength range 1–4  $\mu\text{m}$  and with spectral widths 5– $10 \times 10^{-3}$   $\mu\text{m}$  gives variations in apparent size from 36 mas to 62 mas (Woodruff et al. 2008, 2009). Measurements of the radio continuum at 7 mm wavelength show a somewhat irregular shape which is fitted with an ellipse that has a maximum diameter of 0'.069 and a minimum of 0'.046 (Reid & Menten 2007). Radiation measured in this case is presumably due to  $\text{H}^-$  and  $\text{H}_2^-$  free-free emission. Cotton et al. (2008) have measured a ring of SiO maser emission surrounding W Hydrae with a diameter of  $\sim 70$  mas, which would represent an upper limit to the stellar diameter. The dust envelope has been previously measured at 18  $\mu\text{m}$  (Marengo et al. 2000) to have an oval shape with FWHM size of 0'.5 (R.A.)  $\times$  0'.8 (decl.) (M. Marengo 2009, private communication). This star and its surroundings are clearly complex. Present measurements use an assumed stellar diameter of 50 mas to provide characteristics specifically of the dust which surrounds W Hydrae. These measurements should be rather reliable because of the narrow bandwidth which avoids possible confusion due to spectral lines of molecular gas.

K. Reichl, C. S. Ryan, J. Chu, D. D. S. Hale, and W. Fitelson gave excellent assistance during the measurements published here, and their help is much appreciated. The luminosity period was obtained using data from the All Sky Automated

Survey (ASAS) and the American Association of Variable Star Observers (AAVSO). This work also made use of the SIMBAD database. Fitting programs used the mpfit IDL routines of C. B. Markwardt. We are grateful for support from the Gordon and Betty Moore Foundation, the Office of Naval Research, and the National Science Foundation.

#### REFERENCES

- Cotton, W. D., Perrin, G., & Lopez, B. 2008, *A&A*, 477, 853  
Hale, D. D. S., et al. 2000, *ApJ*, 537, 998  
Marengo, M., Fazio, G. G., Hora, J. L., Hoffman, W. F., Dayal, A., & Deutch, L. K. 2000, in ASP Conf. Ser. 199, Asymmetrical Planetary Nebulae II: From Origins to Microstructures, ed. J. H. Kastner, N. Soker, & S. Rappaport (San Francisco, CA: ASP), 91  
Monnier, J. D., Geballe, T. R., & Danchi, W. C. 1998, *ApJ*, 502, 833  
Monnier, J. D., et al. 2004, *ApJ*, 605, 434  
Reid, M. J., & Menten, K. M. 2007, *ApJ*, 671, 2068  
Tatebe, K., Chandler, A. A., Hale, D. D. S., & Townes, C. H. 2006, *ApJ*, 652, 666  
Whitelock, P. A., Feast, M. W., & van Leeuwen, F. 2008, *MNRAS*, 386, 313  
Woodruff, H. C., Ireland, M. J., Tuthill, P. G., Monnier, J. D., Bedding, T. R., Danchi, W. C., Scholz, M., Townes, C. H., & Wood, P. R. 2009, *ApJ*, 691, 1328  
Woodruff, H. C., Tuthill, P. G., Monnier, J. D., Ireland, M. J., Bedding, T. R., Lacou, S., Danchi, W. C., & Scholz, M. 2008, *ApJ*, 673, 418